

interpretation consistent with the data suggests that the intercalator portion of MPE "delivers" the iron/oxygen chemistry to the DNA helix.

**Acknowledgment.** We are grateful to the National Institutes of Health for grant support (GM27681) and a National Research Service Award (GM 07616) to R.P.H.

**Registry No.** 1, 80082-09-3; 2, 66442-94-2; 3, 80082-10-6; MPE-Fe(II), 80105-72-2; MPE-Ni(II), 80105-73-3; MPE-Zn(II), 80105-74-4; EDTA-Fe(II), 15651-72-6; Fe, 7439-89-6; 1,3-diaminopropane, 109-76-2; EDTA, 60-00-4.

### Crystal and Molecular Structure of the Isobacteriochlorin 3,7-Dimethyl-3',7'-dihydro-2,2',8,8',12,13,17,18-octaethylporphyrin. A Model for Sirohydrochlorin and Siroheme

K. M. Barkigia,<sup>\*1a</sup> J. Fajer,<sup>1a</sup> C. K. Chang,<sup>1c</sup> and G. J. B. Williams<sup>1b</sup>

Department of Energy and Environment  
and the Chemistry Department  
Brookhaven National Laboratory, Upton, New York 11973  
and the Department of Chemistry  
Michigan State University, East Lansing, Michigan 48824

Received September 18, 1981

In addition to the well-established roles of chlorophylls and bacteriochlorophylls in photosynthesis,<sup>2</sup> an increasing body of evidence indicates that reduced porphyrins also mediate diverse biological functions such as catalytic decomposition of peroxide<sup>3</sup> as well as assimilatory and dissimilatory reductions of nitrites and sulfites.<sup>4</sup> The prosthetic groups of sulfite and nitrite reductases, enzymes which catalyze the six-electron reductions of sulfite and nitrite to H<sub>2</sub>S and NH<sub>3</sub>, respectively, have been characterized as iron isobacteriochlorins or sirohemes (1). The demetalated form of siroheme, sirohydrochlorin, has been further identified as a precursor to vitamin B<sub>12</sub> and thus may intriguingly bridge the evolutionary roles of the porphyrin and corrin macrocycles.<sup>5</sup>

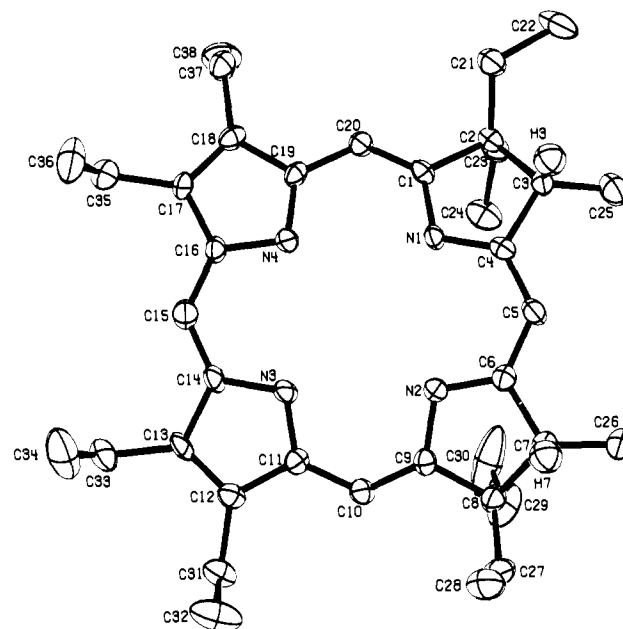
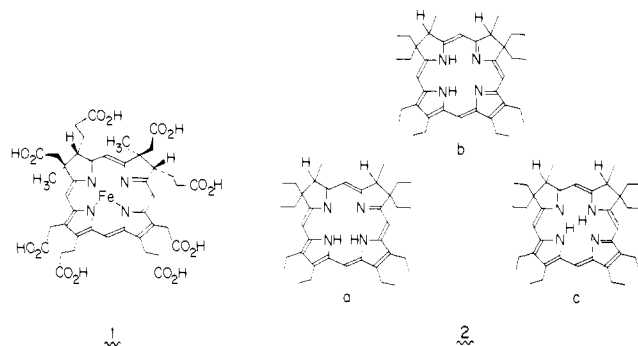


**Figure 1.** Structure of **2** and atom-numbering system. The hydrogen atoms are numbered according to the carbon atom to which they are bonded. The thermal ellipsoids are drawn to enclose 30% probability. Hydrogen atoms other than those on rings I and II are omitted for clarity.

Considerable attention is now focused on the synthesis of isobacteriochlorins (iBC)<sup>6-11</sup> and their theoretical,<sup>12</sup> structural,<sup>13,14</sup> and chemical<sup>6-14</sup> properties as guides to the chemistry of siroheme and sirohydrochlorin in vivo. We present here an X-ray determination of dimethyloctaethylisobacteriochlorin (**2**), a compound which is spectroscopically similar to sirohydrochlorin and bears a substituent pattern more akin to that found in vivo than other sirohydrochlorin analogues synthesized recently. This pattern was deliberately chosen<sup>6</sup> to mimic the resistance of siroheme and sirohydrochlorin to oxidative dehydrogenation of the two reduced pyrroles.

The structure of **2**, along with atom names, is displayed in Figure 1. The compound crystallizes<sup>15</sup> in a unit cell comprised

(5) Scott, A. I.; Irwin, A. J.; Siegel, L. M.; Shoolery, J. N. *J. Am. Chem. Soc.* **1978**, *100*, 316-318; 7987-7994. Scott, A. I. *Acc. Chem. Res.* **1978**, *11*, 29-36. Battersby, A. R.; Jones, K.; McDonald, E.; Robinson, J. A.; Morris, H. R. *Tetrahedron Lett.* **1977**, 2213-2216. Battersby, A. R.; McDonald, E.; Morris, H. R.; Thompson, M.; Williams, D. C.; Bykhovsky, V. Ya.; Zaitseva, N. I.; Bukin, V. N. *Ibid.* **1977**, 2217-2220. Battersby, A. R.; McDonald, E.; Thompson, M.; Bykhovsky, V. Ya. *J. Chem. Soc., Chem. Commun.* **1978**, 150-151.

(6) Chang, C. K.; Fajer, J. *J. Am. Chem. Soc.* **1980**, *102*, 848-851.  
(b) Chang, C. K. *Biochemistry* **1980**, *19*, 1971-1976.

(7) Harel, Y.; Manassen, J. *J. Am. Chem. Soc.* **1977**, *99*, 5817-5818.

(8) Stolzenberg, A. M.; Spreer, L. O.; Holm, R. H. *J. Chem. Soc., Chem. Commun.* **1979**, 1077-1078. *J. Am. Chem. Soc.* **1980**, *102*, 364-370. Stolzenberg, A. M.; Strauss, S. M.; Holm, R. H. *Ibid.* **1981**, *103*, 4763-4775.

(9) Ulman, A.; Gallucci, J.; Fisher, D.; Ibers, J. A. *J. Am. Chem. Soc.* **1980**, *102*, 6852-6854.

(10) Montforts, F. P.; Ofner, S.; Rasetti, V.; Eschenmoser, A.; Waggon, W. D.; Jones, K.; Battersby, A. R. *Angew. Chem., Int. Ed. Engl.* **1979**, *18*, 675-677. Harrison, P. J.; Fookes, C. J. R.; Battersby, A. R. *J. Chem. Soc., Chem. Commun.* **1981**, 797-799.

(11) Angst, C.; Kajiwara, M.; Zass, E.; Eschenmoser, A. *Angew. Chem., Int. Ed. Engl.* **1980**, *19*, 140-141. Naab, P.; Lattman, R.; Angst, C.; Eschenmoser, A. *Ibid.* **1980**, *19*, 143-145.

(12) Richardson, P. F.; Chang, C. K.; Spaulding, L. D.; Fajer, J. *J. Am. Chem. Soc.* **1979**, *101*, 7736-7738. Richardson, P. F.; Chang, C. K.; Hanson, L. K.; Spaulding, L. D.; Fajer, J. *J. Phys. Chem.* **1979**, *83*, 3420-3424. Chang, C. K.; Hanson, L. K.; Richardson, P. F.; Young, R.; Fajer, J. *Proc. Natl. Acad. Sci. U.S.A.* **1981**, *78*, 2652-2656.

(13) Barkigia, K. M.; Fajer, J.; Spaulding, L. D.; Williams, G. J. B. *J. Am. Chem. Soc.* **1981**, *103*, 176-181.

(14) Kratky, C.; Angst, C.; Eigill, J. *Angew. Chem., Int. Ed. Engl.* **1981**, *20*, 211-212.

(1) (a) Department of Energy and Environment. (b) Chemistry Department, BNL. (c) Michigan State University.

(2) Clayton, R. K.; Sistrom, W. R., Eds. *"The Photosynthetic Bacteria"*; Plenum Press: New York, 1978. Govindjee, Ed. *"Bioenergetics of Photosynthesis"*; Academic Press: New York, 1975. Olson, J. M.; Hind, G., Eds. *Brookhaven Symp. Biol.* **1976**, *28*.

(3) Jacob, G. S.; Orme-Johnson, W. H. *J. Biol. Chem.* **1979**, *18*, 2967-2980.

(4) Horie, S.; Watanabe, T.; Nakamura, S. *J. Biochem.* **1976**, *80*, 579-593. Siegel, L. M.; Murphy, M. J.; Kamin, H. *J. Biol. Chem.* **1973**, *248*, 251-264. Murphy, M. J.; Siegel, L. M.; Kamin, H. *Ibid.* **1973**, *248*, 2801-2814. Murphy, M. J.; Siegel, L. M.; Tove, S. R.; Kamin, H. *Proc. Natl. Acad. Sci. U.S.A.* **1974**, *71*, 612-616. Vega, J. M.; Garrett, R. H. *J. Biol. Chem.* **1975**, *250*, 7980-7989. Huckelsby, D. P.; James, D. M.; Banwell, M. J.; Hewitt, E. J. *Phytochemistry* **1976**, *15*, 599-603.

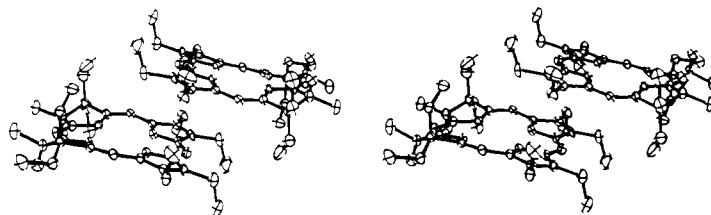


Figure 2. Stereoscopic view of **2** which illustrates the overlap of rings III of inversion-related molecules.

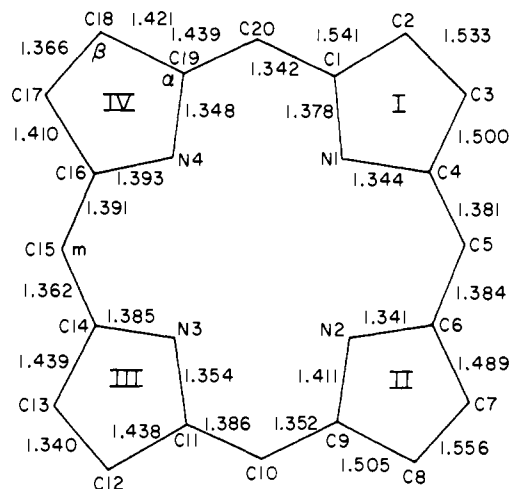


Figure 3. Bond distances (Å) for the core of **2**. The esd are 0.007 Å for C–N bonds and 0.008 Å for C–C bonds.

of two molecules in which pyrrole rings III of inversion-related molecules overlap with a separation of 3.82 Å, indicative of  $\pi$ – $\pi$  interactions (Figure 2). This arrangement appears to minimize steric hindrance of the ethyl substituents. As shown in Figure 3, the bond distances reflect almost mirror symmetry across an imaginary line through C5 and C15 and clearly demonstrate that the macrocycle contains the two adjacent sets of saturated and unsaturated pyrrole rings characteristic of iBCs.

A salient feature of the geometry of **2** is the distortion of the reduced rings. The  $C_{\alpha}C_{\beta}C_{\gamma}C_{\delta}$  torsion angles in rings I and II are 24.1 (3) and  $-24.5^{\circ}$ , respectively, as opposed to  $-0.6$  and  $-1.4^{\circ}$  in rings III and IV. Both methyl carbons C25 and C27 are equatorial to the plane of the macrocycle, while H3 and H7 sit axially above the ring, on either side of the pseudo mirror plane. Rings III and IV are individually planar to 0.01 Å while in I and II the deviations of all carbon atoms from the plane of each ring are substantial. The displacement of all atoms from the plane of the four nitrogens (Figure 4) further illustrates the nonplanarity of the macrocycle.

The four nitrogens are quite planar and form a rectangular cavity at the center of the macrocycle. The distances of N1 and N2 to the centroid of 2.030 and 2.053 Å are markedly shorter than those of N3 and N4, which are 2.081 and 2.080 Å, respectively. Within the precision of this study, the  $C_{\alpha}$ –N– $C_{\alpha}$  angles at N2 ( $109.0^{\circ}$ ) and N3 ( $109.2^{\circ}$ ) are equal, with that at N1 the largest,  $110.7^{\circ}$ , and at N4 the smallest,  $105.6$  (5) $^{\circ}$ .

(15) Compound **2**,  $C_{38}N_4H_{54}$ , crystallizes from toluene/methanol with  $Z = 2$  in the triclinic space group  $P1$  in a cell of dimensions  $a = 12.300$  (9) Å,  $b = 13.998$  (4) Å,  $c = 11.392$  (6) Å,  $\alpha = 109.78$  (3) $^{\circ}$ ,  $\beta = 95.37$  (5) $^{\circ}$ ,  $\gamma = 68.69$  (3) $^{\circ}$ ,  $V = 1718.4$  Å<sup>3</sup>. A sphere of data was obtained on an Enraf-Nonius CAD4 diffractometer with graphite monochromated Cu K $\alpha$  radiation in the scan range,  $0 \leq 2\theta \leq 100^{\circ}$ . Of the 8248 reflections collected, symmetry equivalents were averaged to give 3524 unique and 2041 with  $F_0 \geq 2\sigma(F_0)$ . An anisotropic model was refined by least squares to  $R_F = 0.092$  and  $R_{WF} = 0.082$ . Because of the large number of variable parameters, two matrix blocks were used: one consisted of the overall scale and the positional and thermal parameters for the core and the second contained the scale and the positional and thermal parameters for the side chains. All hydrogens were located but their positions were idealized 0.95 Å away from their respective carbon or nitrogen in the final cycles of refinement. Each hydrogen was assigned a  $B$  of 6.0 Å<sup>2</sup>.

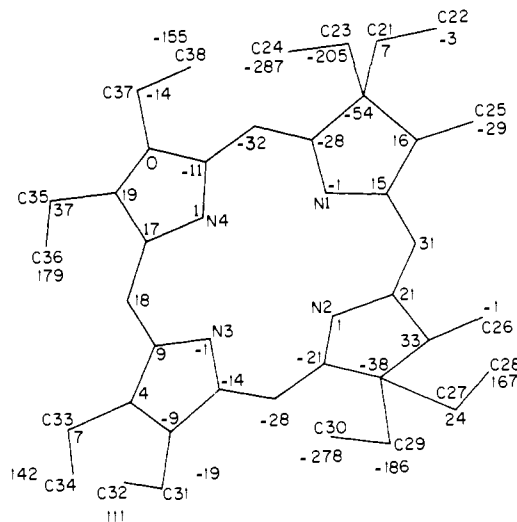


Figure 4. Deviations ( $\text{Å} \times 10^2$ ) from the least-squares plane of the four nitrogens. The average uncertainty is 0.01 Å.

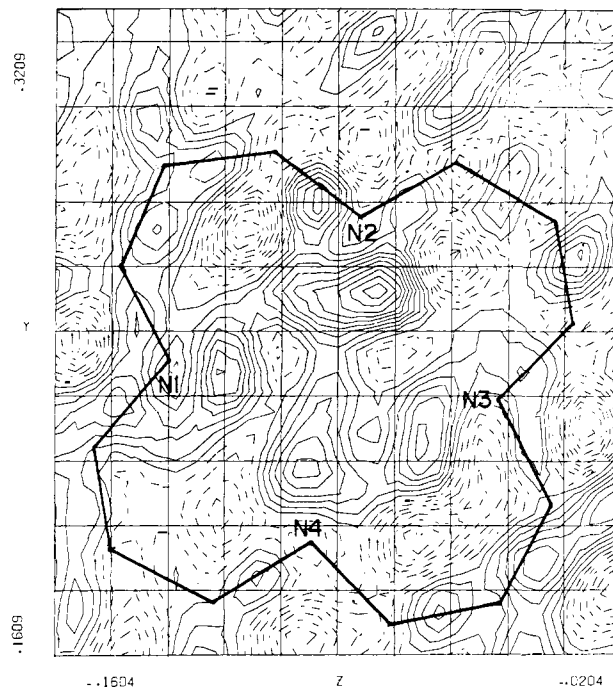


Figure 5. Difference electron density map in the plane of the four nitrogens. The contour intervals are shown in arbitrary units of 100 with negative density indicated by broken lines. The four central peaks range from 0.20 to 0.29  $e/\text{Å}^3$ . The heavy line traces the pyrrole nitrogens and the  $\alpha$  and methine carbons.

Difference electron density maps of the central cavity reveal the inner protons as maxima ranging from 0.2 to 0.3  $e/\text{Å}^3$  distributed over the four nitrogens (Figure 5). These results imply multiple tautomeric forms of **2** in which the protons are localized on adjacent or opposite rings. Infrared and optical studies of **2** as a function of temperature and solvent<sup>6b</sup> also provide evidence of tautomerization and suggest that the process is dynamic rather

than static.  $^1\text{H}$  NMR data<sup>16</sup> indicate that the ring current in isobacteriochlorins is lower than in bacteriochlorins, chlorins, or porphyrins in accord with a lower degree of aromaticity and thus with tautomers in which the conjugation is interrupted (**2b** and **c**). The bond distances observed in **2** (Figure 3) support such a disruption.

The emerging structural data for chlorins,<sup>9,17</sup> bacteriochlorins,<sup>18</sup> and isobacteriochlorins<sup>13,14</sup> indicate that the reduced rings of the macrocycles are flexible and can assume a wide range of conformations, influenced in part by the occupancy of the porphyrin pocket. Zn(II) complexes exhibit<sup>13</sup> only moderate deviations of the macrocycles from planarity whereas nickel(II) chlorins<sup>9</sup> and isobacteriochlorins<sup>14</sup> are particularly distorted. ESR results for cation radicals of **2** and its Zn and hexacoordinated Fe(II) complexes, which probe the  $\beta$  protons of the reduced rings and their spatial interactions with the  $\alpha$  carbons, reveal no major differences between the three compounds.<sup>12,19</sup> This constancy implies that the average conformations of the ligands in solution are similar. Extrapolation of the model studies to the biological pigments suggests therefore that sirohydrochlorin and low-spin iron(II) siroheme should exhibit comparable conformational profiles.

In a different context, the present results may also be relevant to the "special pairs" of bacteriochlorophylls that act as light traps and primary electron donors in bacterial photosynthesis.<sup>20</sup> As in iBC cation radicals,<sup>12</sup> the HOMOs of bacteriochlorophyll cations localize unpaired spin at the reduced rings with the result that the observed ESR and ENDOR parameters of the radicals depend heavily on the orientations of these rings.<sup>21</sup> Conformational changes in the flexible reduced rings, induced by the "special pair" packing and/or protein interactions, thus provide an attractive structural explanation for the variety of ESR and ENDOR data observed for bacteriochlorophyll radicals in vivo.<sup>20-22</sup>

**Note Added in Proof.** The structure of another isobacteriochlorin, 3,3',7,7'-tetrahydro-2,2',8,8',12,13,17,18-octamethylporphyrin, has recently been solved.<sup>23</sup> As in the present work, the central protons are delocalized, and an interrupted conjugative path is indicated. In sharp contrast to the results presented here, the molecule is planar and thus further illustrates the wide range of conformations that reduced porphyrins can assume.

**Acknowledgment.** This work was supported by the Division of Chemical Sciences, U.S. Department of Energy, under Contract DE-AC02-76CH00016 at Brookhaven National Laboratory and U.S. Department of Agriculture Grant 59-2261-0-1-437-0 at Michigan State University. We thank Dr. O. Kennard for disclosure of results prior to publication.

**Registry No.** **2a**, 80106-11-2; **2b**, 80106-12-3; **2c**, 72218-67-8.

**Supplementary Material Available:** Crystallographic details, selected bond angles, bond distances in the side chains, least-squares planes, atom coordinates and anisotropic vibrational parameters for the nonhydrogen atoms, coordinates of the hydrogen atoms, and a listing of structure amplitudes (20 pages). Ordering information is given on any current masthead page.

(16) Harel, Y.; Manassen, J. *Org. Magn. Reson.* **1981**, *15*, 1-6.

(17) Spaulding, L. D.; Andrews, L. C.; Williams, G. J. B. *J. Am. Chem. Soc.* **1977**, *99*, 6918-6923. Serlin, R.; Chow, H. C.; Strouse, C. E. *Ibid.* **1975**, *97*, 7237-7242. Fischer, M. S.; Templeton, D. H.; Zalkin, A.; Calvin, M. *Ibid.* **1973**, *94*, 3613-3619. Kratky, C.; Isenring, H. P.; Dunitz, J. D. *Acta Crystallogr., Sect. B* **1977**, *B33*, 547-549 and references therein.

(18) Barkigia, K. M.; Fajer, J.; Smith, K. M.; Williams, G. J. B. *J. Am. Chem. Soc.* **1981**, *103*, 5890-5893.

(19) Richardson, P. F.; Chang, C. K.; Fajer, J., unpublished results. The proton coupling constants of the Zn complex are identical with those of the free base.

(20) Katz, J. J.; Norris, J. R.; Shipman, L. L.; Thurnauer, M. C.; Wasielewski, M. R. *Annu. Rev. Biophys. Bioeng.* **1978**, *7*, 393-434. Feher, G.; Hoff, A. J.; Isaacson, R. A.; Ackerson, L. C. *Ann. N.Y. Acad. Sci.* **1975**, *244*, 239-259.

(21) Davis, M. S.; Forman, A.; Hanson, L. K.; Thornber, J. P.; Fajer, J. *J. Phys. Chem.* **1979**, *83*, 3325-3332.

(22) Lenzian, F.; Lubitz, W.; Scheer, H.; Bubbenzer, C.; Mobius, K. *J. Am. Chem. Soc.* **1981**, *103*, 4635-4637.

(23) Cruse, W. B. T.; Harrison, P. J.; Kennard, O. *J. Am. Chem. Soc.*, in press.

## Trans Lengthening of M-H Bonds and Steric Modification of M-P Bond Lengths in Chloro- and Hydrido-Transition-Metal-Phosphine Complexes

Glen B. Robertson\* and Paul A. Tucker

*Research School of Chemistry  
The Australian National University  
Canberra, ACT 2600, Australia*

*Received August 3, 1981*

In addition to primary metal and ligand types, metal-ligand distances in transition-metal complexes are dependent on a variety of factors, including metal and/or ligand oxidation state, coordination number and geometry, cis- and trans-bond lengthening effects, intramolecular nonbonded interactions, and in the solid state, intermolecular interactions of various types. Recent X-ray and (in some cases) neutron diffraction analyses of members of the series of complexes  $\text{L}_3\text{H}_{3-n}\text{Cl}_n\text{Ir}^{\text{III}}$  [ $\text{L} = \text{PMe}_2\text{Ph}$ ;  $n = 0-3$ ] provide valuable new insight into the relative importance of some of these factors. Relevant bond length data for *mer*- $[\text{L}_3\text{Cl}_3\text{Ir}^{\text{III}}]^1$  (**1**), *mer*- $[\text{L}_3\text{-trans-Cl}_2\text{H}\text{Ir}^{\text{III}}]$  (**2**), *mer*- $[\text{L}_3\text{-cis-Cl}_2\text{H}\text{Ir}^{\text{III}}]$  [monoclinic (**3a**), and orthorhombic (**3b**), modifications], *mer*- $[\text{L}_3\text{Cl-cis-H}_2\text{Ir}^{\text{III}}]$  (**4**), *fac*- $[\text{L}_3\text{Cl}_3\text{Ir}^{\text{III}}]$  (**5**), and *fac*- $[\text{L}_3\text{H}_3\text{Ir}^{\text{III}}]^2$  (**6**) are shown in Table I.<sup>3</sup> Even in this series, and for given ligand type, variable factors will include (as a minimum) the specific nature of the trans ligand, the differing steric requirements of the anionic ligands (Cl or H), ligand-ligand nonbonding interactions, and the intermolecular force fields. Because these factors are interdependent, we are unable to rationalize the variations indicated in Table I in detail. We are able, however, to derive some useful estimates of the relative magnitudes of the various effects.

Complexes **1**, **3a**, and **5**, each crystallize with two molecules per asymmetric unit, and despite the differing crystalline environments of pair members, chemically equivalent metal-ligand bond lengths do not differ significantly.<sup>4</sup> These data suggest an upper limit of ca. 0.005 Å for the effect of the intermolecular force field on the metal-ligand bond lengths. Other effects are much more substantial. Thus, for any particular complex, we observe that the trans influence on metal-ligand bond lengths is marked and that the order ( $\text{H} > \text{PMe}_2\text{Ph} > \text{Cl}$ ) is as expected.<sup>5</sup> As the trans ligand is changed from chloride to phosphine and from phosphine to hydride, Ir-Cl is increased by ca. 0.07 and 0.05 Å respectively. The corresponding increases in Ir-P are ca. 0.10 and 0.04 Å. Trans lengthening of the Ir-H bond is also evident, with substitution of phosphine for chloride, causing an increase in Ir-H of ca. 0.05 Å. The Ir-H lengthening is only a little less than that observed for Ir-Cl with the same ligands. So far as we are aware, the present results provide the first quantitative measure of this effect in simple octahedral systems.

Next, comparison between different *mer* complexes (**1-4**) shows that whereas the Ir-Cl (and Ir-H) bond length trans to a given ligand is approximately constant, the Ir-P bond length trans to a given ligand is certainly not constant. There is a clear trend that, as the degree of hydride substitution is increased by unity, the Ir-P bond length (for any given trans ligand) is decreased by ca. 0.04 Å.<sup>6</sup> The same effect is illustrated dramatically in the *fac* complexes (**5**, **6**) where, despite the marked difference in the

(1) A redetermination of the structure originally reported by: Aslanov, L.; Mason, R.; Wheeler, A. G.; Whimp, P. O. *J. Chem. Soc., Chem. Commun.* **1970**, 30.

(2) Bau, R., private communication, 1978. Bau, R. "Transition Metal Hydrides"; American Chemical Society: Washington, DC, 1978; *Adv. Chem. Ser. No.* 167.

(3) M-H distances are from neutron diffraction data collected at the Australian Atomic Energy Commission (Lucas Heights) with the support of the Australian Institute for Nuclear Science and Engineering and at the Institute Laue-Langevin (Grenoble) with support from the Science Research Council of Great Britain.

(4) Except for Ir-Cl (trans to H) in **3a**. The inequivalence is apparent in both X-ray and neutron refinements. Its origin is not yet clear.

(5) McWeeny, R.; Mason, R.; Towl, A. D. C. *Discuss. Faraday Soc.* **1969**, *47*, 20.

(6) We have already noted (Robertson, G. B.; Tucker, P. A.; Whimp, P. O. *Inorg. Chem.* **1980**, *19*, 2307) that Ir-P bond lengths in hydride complexes of that metal lie at the shorter end of the observed range.